

We are IntechOpen, the world's leading publisher of Open Access books Built by scientists, for scientists

4,800

Open access books available

122,000

International authors and editors

135M

Downloads

Our authors are among the

154

Countries delivered to

TOP 1%

most cited scientists

12.2%

Contributors from top 500 universities



WEB OF SCIENCE™

Selection of our books indexed in the Book Citation Index
in Web of Science™ Core Collection (BKCI)

Interested in publishing with us?
Contact book.department@intechopen.com

Numbers displayed above are based on latest data collected.

For more information visit www.intechopen.com



Polymer/Montmorillonite/Silver Nanocomposite Micro- and Nanoparticles Prepared by *In-Situ* Polymerization and Electrospaying Technique

Jeong Hyun Yeum¹, Jae Hyeung Park¹, Jae Young Choi¹
Jong Won Kim², Sung Kyou Han³ and Weontae Oh⁴

¹*Department of Advanced Organic Materials Science & Engineering,
Kyungpook National University, Daegu,*

²*R&D Division, Korea Dyeing Technology Center, Daegu,*

³*R&D Division, Taihan Textile Co. Ltd., Daegu,*

⁴*Department of Materials and Components Engineering, Dong-eui University, Busan,
Korea*

1. Introduction

Polymer nanocomposite materials have the capacity for producing a synergetic association with surpassing merit properties which cannot be obtained from the individual components. Such materials can be obtained by simply mixing required organic and inorganic components. The introduction of inorganic material into the polymer matrix has proved to be an effective and low-cost method to improve the performance of the existing polymer materials (Okamoto et al., 2000; Ramos et al., 2000; Wu et al., 2006; Zhu et al., 2000). It has various applications, such as new biological materials (biosensors and biochips), biocompatible thin coatings for medical applications, biodegradable scaffolds, drug delivery system and filter systems (Matsumoto et al., 2005; Okuda et al., 1996; Salata et al., 1997; Sinha et al., 2004).

The synthesis of polymer nanocomposites can be carried out by many different methods. For example, in-situ polymerization of monomers inside the galleries of the inorganic host has been one of the common methods for preparation of nanocomposites. Another common methods are based on melt intercalation, solventless melt intercalation, using microwaves, latex-colloid interaction, solvent evaporation, spray drying, shirasu porous glass membrane emulsification technique and electrospaying, etc. (Berkland et al., 2001; Ma et al., 1999; Messersmith et al., 1993; Mu et al., 2001; Oriakhi et al., 1995; Rosca et al., 2004; Usuki et al., 1993). This article is concerned with fabrication of polymer nanocomposite particles by *in-situ* suspension polymerization and electrospaying which are represented as a traditional and current general method for synthesis of nanocomposite. The effectiveness of these nanocomposite particles are demonstrated with a field emission-type scanning electron microscope (FE-SEM), a transmission electron microscopy (TEM), an optical microscope, a reflection type X-ray diffraction (XRD), a

Fourier transform spectroscopy (FT-IR), a thermogravimetric analysis (TGA), a nuclear magnetic resonance Spectrometer ($^1\text{H-NMR}$), and the anti-bacterial performance was also discussed.

2. *In-Situ* suspension polymerization for polymer/silver and polymer/montmorillonite nanocomposite microparticles

For a long time, quite a range of polymer/inorganic nanocomposites have been investigated via *in-situ* suspension polymerization. Using suspension polymerization to prepare polymer/inorganic nanocomposite particle is interesting in terms of an easy manipulation, low cost, and controllable particle size. It is well known that a range of variables, such as the type and amount of initiator and suspending agent, the polymerization temperature, the monomer to water ratio, and the agitation speed, affect the molecular weight of the polymer synthesized (Gotoh et al., 2000; Giannetti et al., 1986; Hatchett et al., 1999; Huang et al., 1991; Lee et al., 2004).

In this section, we are reporting the *in-situ* synthesis of poly(vinyl acetate) (PVAc)/silver (Ag) and poly(vinyl alcohol) (PVA)/PVAc/montmorillonite (MMT) nanocomposite particles using a suspension polymerization technique (Jung et al., 2006; Jung et al., 2007; Yeum et al., 2005). The effects of MMT and Ag on the morphology, size, conversion rate, and polymerization time of nanocomposite particles were examined. According to the inorganic materials and polymerization process, different type of particles such as spherical, rugged surface and golf ball shape microparticles are successfully prepared. The X-ray diffraction analysis illustrated that the clay silicate layer are intercalated in the polymer matrix.

2.1 Experimental

2.1.1 Materials

Vinyl acetate (VAc) purchased from Sigma-Aldrich was washed with an aqueous solution of NaHSO_3 and water, and then dried with anhydrous CaCl_2 followed by distillation under nitrogen atmosphere at a reduced pressure. The initiator, 2,2'-azobis (2,4-dimethylvaleronitrile) (ADMVN) (Wako Co.) was recrystallized twice in methanol before use. PVA with number average molecular weight of 127,000 and degree of saponification of 88% (Aldrich Co.) was used as a suspending agent. Aqueous Ag nanoparticles dispersion (AGS-WP001, 10 000 ppm) with diameters ca. 15–30 nm were purchased from Miji Tech. Co., Ltd., Korean. Pristine Na-MMT, Kunipia-F from Kunimine, Japan, was used as received. It consists of exchangeable sodium ions with cationic exchange capacity of ca. 119 meq/100 g. The average particle size and surface area of Na-MMT were 100–1,000 nm and 750 m^2/g , respectively. Polyethylene glycol dipolyhydroxystearate (Arlacel P135), purchased from Uniquema, and cationic surfactant, such as cetyltrimethylammonium bromide (CTAB), obtained from Aldrich, are used as surfactants in order to disperse the Ag and MMT in polymer matrix, respectively. Deionized water was used for all of the experiments.

2.1.2 Preparation of PVAc/Ag nanocomposite microparticles

To prepare PVAc/Ag nanocomposite microparticles, a suspension polymerization approach in the presence of aqueous Ag nanoparticle was used. The polymerization was conducted in a 250 ml three-neck round bottom flask fitted with a condenser. In a typical run, the

suspending agent was first dissolved in water under nitrogen atmosphere with constant stirring. Surfactant was dissolved in VAc monomer. After the surfactant was dissolved, Ag nanoparticle in water suspension and desired initiator was mixed with VAc monomer under ultrasonification for 5 min using Bandelin UW 3,100 equipment. The above mixture was poured into a flask and charged at once at a fixed polymerization temperature. After prefixed reaction time, the reaction liquor was cooled and kept for more than 24 h to allow complete sedimentation of PVAc/Ag nanocomposite microparticles. The PVAc/Ag nanocomposite microparticles were then filtered and washed with warm water to eliminate residual VAc and suspending agent, and dried under vacuum. Conversion was calculated by gravimetric method. In the case of calculating of conversion, weight of Ag was ignored because the total weight of used Ag nanoparticles is less than 0.5% of polymer weight. Conversions were averages of three measurements. The detailed polymerization conditions are listed in Table 1.

2.1.3 Preparation of PVA/PVAc/MMT nanocomposite microparticles

Suspending agent was dissolved in water under a nitrogen atmosphere with constant stirring in a 250 ml reactor fitted with a condenser. CTAB was mixed with the MMT in the monomer phase prior to suspension polymerization. The ADMVN was added at a fixed polymerization temperature. After predetermined times, the reaction mixture was cooled and kept for 24 h to allow the precipitation and separation of the PVAc/MMT nanocomposite microparticles. The collected PVAc/MMT nanocomposite microparticles were further washed with warm water. Conversion was calculated by measuring the weight of the PVAc/MMT using the average value from three determinations. The detailed polymerization conditions are listed in Table 1.

Condition	PVAc/Ag	PVA/PVAc/MMT
Type of initiator	ADMVN	ADMVN
Type of suspending agent	PVA	PVA
Initiator concentration	10 ⁻⁴ , 5x10 ⁻⁴ , 10 ⁻³ mol/mol of VAc	10 ⁻⁴ , 5x10 ⁻⁴ , 10 ⁻³ mol/mol of VAc
Suspending agent concentration	1.5, 5, 9 g/dl of water	1.5 g/dl of water
VAc/water	0.5 l/l	0.5 l/l
Rpm	500	500
Temperature	30, 40, 50 °C	30, 40, 50 °C
Inorganic material concentration	3 wt.% of VAc	1 wt.% of VAc
Surfactant concentration	0, 0.06 wt.% of VAc	0.5 wt.% of VAc

Table 1. Reaction conditions for the suspension polymerization

2.1.4 Heterogeneous saponification of PVA/PVAc/MMT nanocomposite microparticles

To prepare PVA/PVAc/MMT nanocomposite microparticles, heterogeneous saponification of PVAc/MMT nanocomposite microparticles was conducted in a flask equipped with a reflux condenser, a thermocouple, a dropping funnel, and a stirring device. The alkali solution used

for saponification contains 10 g of sodium hydroxide, 10 g of sodium sulfate, 10 g of methanol and 100 g of water. The prepared PVAc/MMT nanocomposite microparticles were slowly added into the alkali solution at 50 °C with gentle stirring. The saponification was stopped at the required time and a PVA shell was formed on the surface of the PVAc/MMT microparticles. After the required reaction time, the mixture was poured into cold water and kept for 1 day to allow the precipitation of spherical core/shell PVA/PVAc/MMT nanocomposite microparticles. Finally, the solid saponification product was filtered and washed several times with water and dried in a vacuum at 40 °C for 1 day.

2.1.5 Characterizations

The morphology of nanocomposite microparticles were examined using a SEM (Hitachi S-570). To obtain the average size and size distribution, five SEM photographs and more than 200 particles were collected by computer, which linked with the SEM, followed by statistical analysis of data by computer. FT-IR spectrum of the sample was obtained using a Perkin-Elmer 1650 that cast on potassium bromide. XRD measurements were performed at room temperature on a Rigaku (D/Max IIIB) X-ray diffractometer using Ni-filtered $\text{CuK}\alpha$ ($\lambda=1.54 \text{ \AA}$) radiation. The core/shell structure of PVA/PVAc/MMT nanocomposite microparticles was examined using an optical microscope (Leica DC 100). The degree of saponification (DS) of PVA/PVAc/MMT nanocomposite microparticles was determined by the ratio of methyl and methylene proton peaks in the $^1\text{H-NMR}$ spectrometer (Varian, Sun Unity 300).

2.2 Results and discussion

2.2.1 PVAc/Ag nanocomposite microparticles

2.2.1.1 Suspension polymerization behaviour

Figure 1(a,b,c) presents the conversion-time relationship at different polymerization temperatures with initiator concentration at 10^{-4} mol/mol of VAc. Generally speaking, the reaction conversion increased with increasing polymerization temperature, regardless of the presence of Ag nanoparticles. Although a low initiator concentration (10^{-4} mol/mol of VAc) was used, the conversion increased steadily with the reaction time at a reaction temperature of 30 °C until ca. 95% of conversion was arrived. In contrary, such a high conversion is impossible in the bulk polymerization of PVAc. The high molecular weight and high conversion obtained suggest that the chain transfer and termination reactions were not significant at the conditions used in this study. As the slope of the curve on the conversion-time plot represents the polymerization rate, the bigger the slope (steeper), the higher the polymerization rate. As can be seen from Figure 1, the introduction of unmodified silver nanoparticles into the system slightly decreased the polymerization rate, in comparison with the absence of them. Otherwise, the rates of polymerization with modified silver nanoparticles are slightly higher than these without silver nanoparticles. The actual reason for the increase in the polymerization rate when the silver nanoparticles were dispersed in the water phase, but the decrease in the polymerization rate when the silver nanoparticles were dispersed in monomer phase is not clear and more work is needed (Lee et al., 2008; Yeum et al., 2005; Yeum et al., 2005). As shown in Figure 1(d,e,f), the polymerization rate, at a reaction temperature of 30 °C, increased with increasing initiator concentration, in accordance with theoretical prediction (O'dian, 1981).

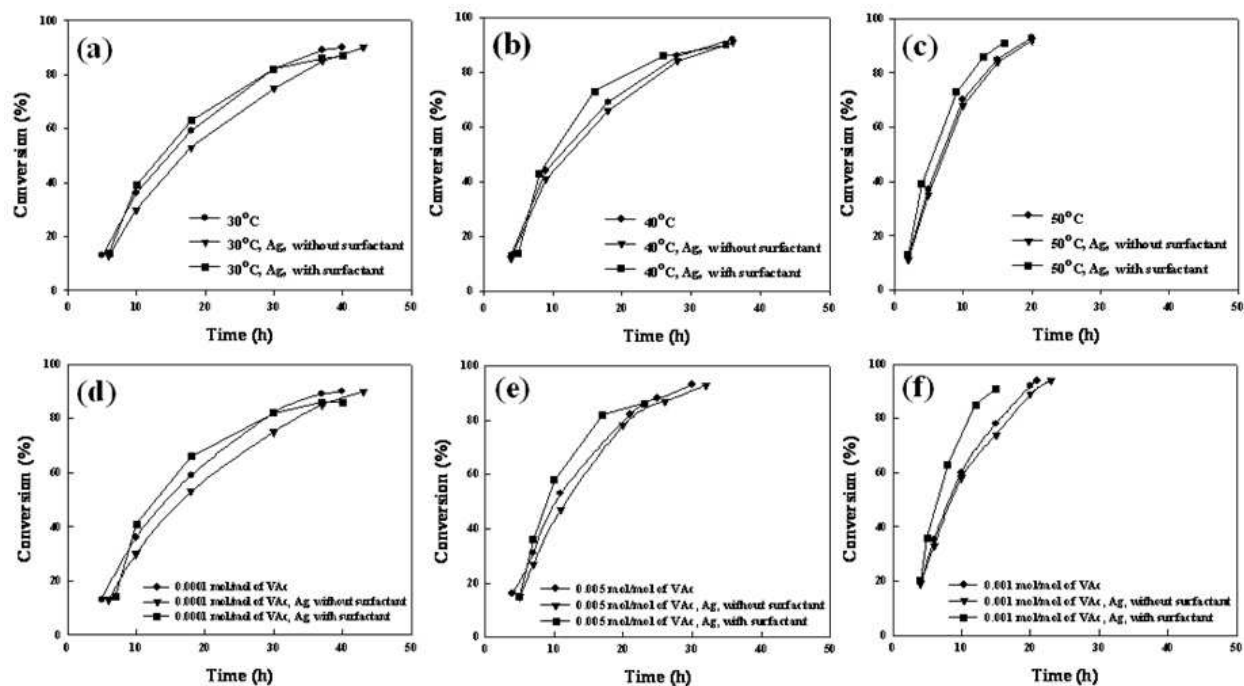


Fig. 1. Conversion vs. polymerization time (a,b,c) at different polymerization temperatures with [ADMVN]= 10^{-4} mol/mol of VAc and (d,e,f) at different [ADMVN] with reaction temperature at 30 °C. (suspending agent concentration: 1.5 g/dl of water)

2.2.1.2 Morphology and structure property

SEM photographs of (a) pure PVAc microparticles, (b) PVAc/Ag nanocomposite microparticles without surfactant and (c) PVAc/Ag nanocomposite microparticles with surfactant suspension-polymerized with a suspending agent concentration of 5.0 g/dl of water are presented in Figure 2, respectively. It is surprising that three different appearances of microparticles, one with smooth surface, and another with rugged surface and the other with golf ball shape were observed. From the SEM observation, it is estimated that ca. 10-20% of particles when polymerized without surfactant are rugged surface. We believe this phenomenon must be related to the aggregation of Ag nanoparticles during the polymerization. It should be noted that the Ag nanoparticles used in this study are in an aqueous suspension form, so the Ag nanoparticles are relatively hydrophilic. For this reason, the Ag particles aggregate to small clusters when they are encapsulated in polymer phase. If these aggregated silver particles stay on the surface of the polymer microparticles, rugged microparticles may be obtained. On the other hand, PVAc/Ag nanocomposite microparticles which were polymerized with modified Ag nanoparticles have golf ball shape. Because of the low hydrophile-lyophile balance number of Arlacel P135, the surface of the Ag nanoparticles was converted from hydrophilic to hydrophobic by the adsorption of Arlacel P135, which resulted in a good dispersion of the Ag nanoparticles in monomer droplets and polymer matrix. The detailed mechanism, such as why PVAc/Ag nanocomposite microparticles have different appearances according to surfactant, is shown in Figure 3. But the reason why only about 10-20% of the microspheres are in rugged surface, is not clear. Further work in this area definitely is needed.

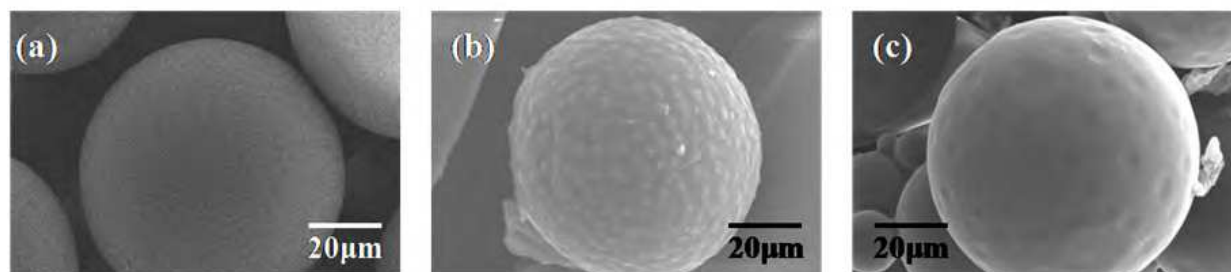


Fig. 2. SEM images of (a) pure PVAc microparticles, (b) PVAc/Ag nanocomposite microparticles without surfactant and (c) PVAc/Ag nanocomposite microparticles with surfactant (ADMVN concentration of 10^{-4} mol/mol of VAc, suspending agent concentration of 5.0 g/dl of water)

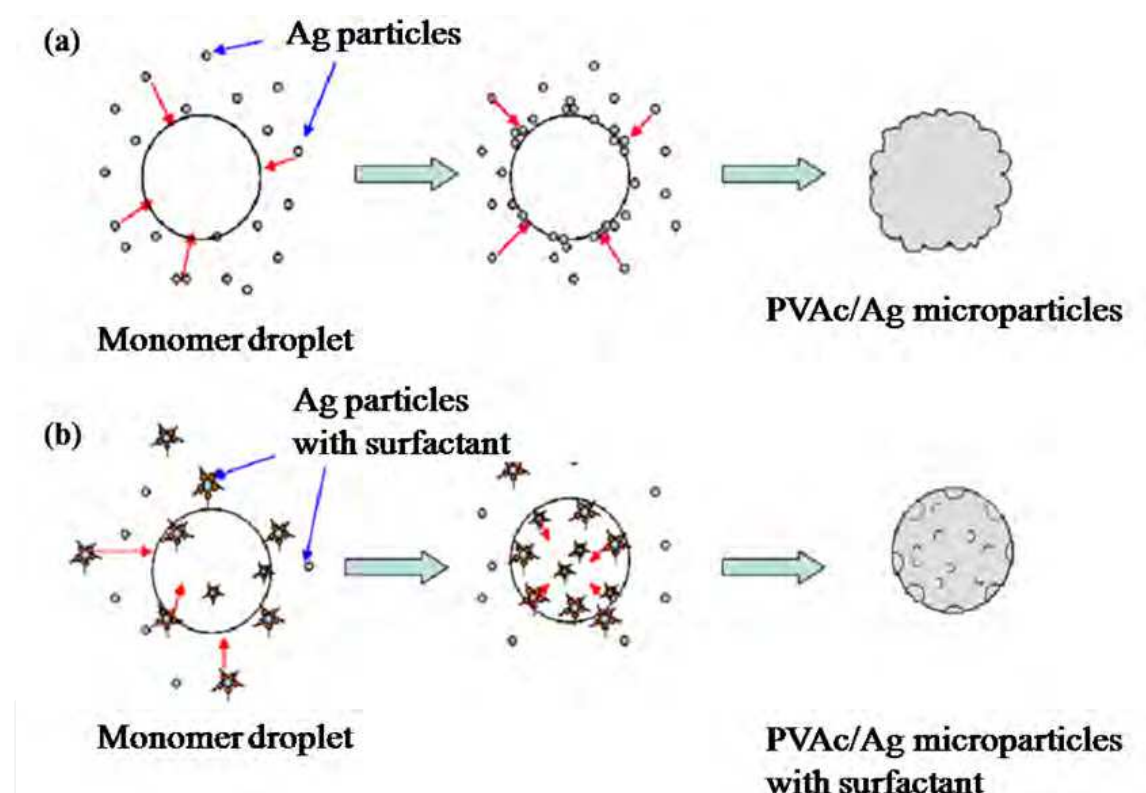


Fig. 3. Schematics of suspension polymerization of PVAc/Ag nanocomposite microparticles (a) without surfactant and (b) with surfactant

The PVAc microparticles and PVAc/Ag nanocomposite microparticles with modified silver nanoparticle contents of 3 wt% were characterized by XRD, and the results are shown in Figure 4. The XRD pattern of PVAc/Ag nanocomposite microparticles shows diffraction peaks at 2θ of ca. 15° , 22.7° , 38.2° , 44.6° , and 52° , respectively. Except the diffraction peaks of PVAc (15° , 22.7°), all the other peaks are corresponding to the silver phase. The XRD pattern clearly indicates that PVAc/Ag nanocomposite microparticles were successfully prepared with modified silver nanoparticles. These peaks are corresponding to the (111) and (200) planes of the silver nanocrystals with cubic symmetry (Dong et al., 2002). XRD results indicate that modified Ag nanoparticles are well dispersed in the PVAc matrix.

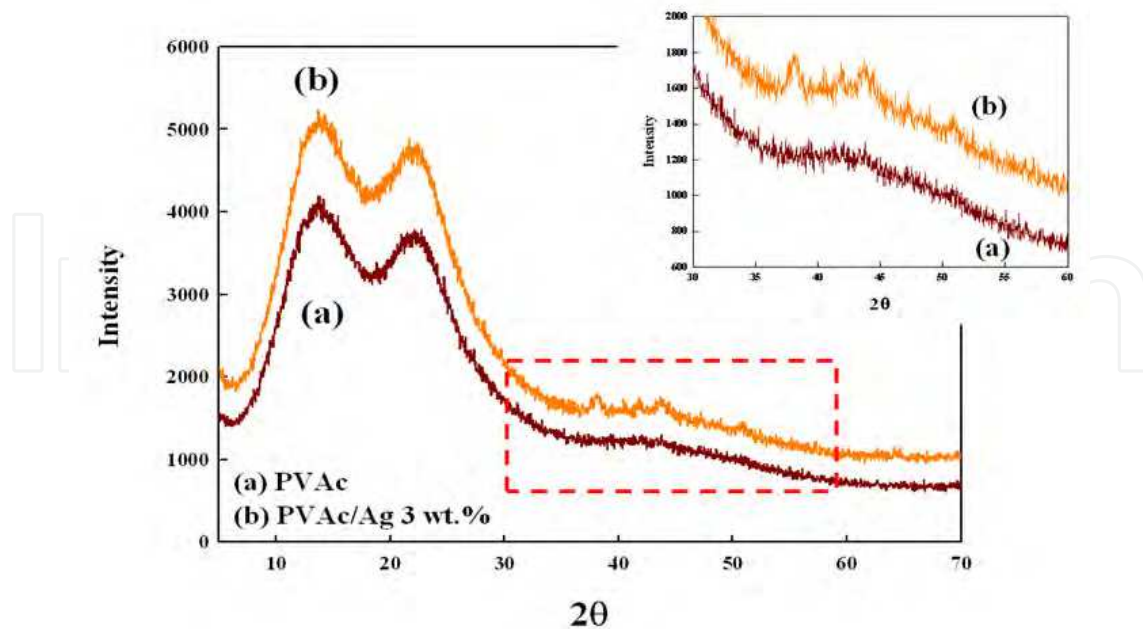


Fig. 4. XRD patterns of (a) pure PVAc and (b) PVAc/Ag nanocomposite microparticles with surfactant

2.2.2 PVA/PVAc/MMT nanocomposite microparticles

2.2.2.1 Suspension polymerization behavior

Figure 5(a) presents the conversion of the polymerization as a function of reaction time in the presence of MMT. The initiator concentration used in these reactions is 10^{-4} mol/mol of VAc. The results indicate that the rate of the polymerization decreased with increasing MMT addition. The reduction in the polymerization rate is probably due to the reduction of the diffusion rate of both monomer molecules and polymer chains in the intergalleries of nanoclay particles. For the polymerization without MMT, Figure 5(a) indicates that the conversion of the polymerization continually increased up to ~40 h, and reached a conversion of ~90% in spite of the low polymerization temperature (30 °C), which suggests that ADMVN is an effective initiator for low-temperature polymerization.

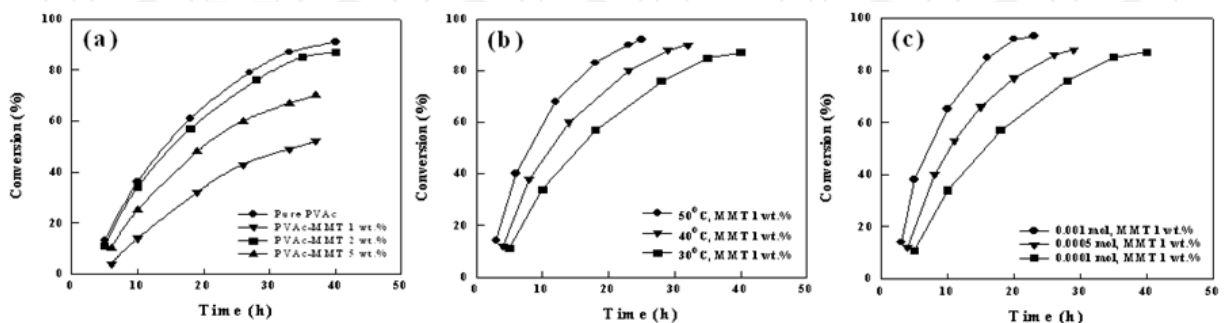


Fig. 5. Conversions of VAc into PVAc/MMT suspension polymerized using ADMVN concentration of 0.0001 mol/mol of VAc (a) with different MMT contents, (b) with different polymerization temperatures, and (c) suspension polymerized using 30 °C with different initiator concentrations with polymerization time, respectively

In a free radical polymerization, the rate of polymerization(R_p) could be expressed by Eq. (1)

$$R_p = K_p[M][I]^{0.5}(fk_d/k_t)^{0.5} \quad (1)$$

where f is the initiator efficiency; $[M]$ and $[I]$ are the concentrations of monomer and initiator; and k_d , k_p , and k_t are the rate constants of initiator decomposition, polymer propagation, and termination, respectively (Odian, 1981). This expression predicts that the rate of polymerization increases as the efficiency and concentration of the initiator are increased. The reduction in the polymerization rate in the presence of MMT suggests that either the efficiency of the initiator, f , or the propagation rate constant, k_p , were decreased when MMT was added into the suspension polymerization system. We believe the reduction of the diffusion rate in the nanoclay intergalleries may reduce both f and k_p in Eq. 1. It has been known that ADMVN is an effective low temperature initiator (the 10h half-life decomposition temperature of ADMVN is 51 °C) for preparing highmolecular-weight polymer with high yield. In this study, ADMVN was used for preparing PVAc/MMT nanocomposite microspheres at room temperature. Figure 5(b) presents the conversion-time relationship for the reactions carried at different temperatures with a constant initiator concentration. Although a low initiator concentration (10^{-4} mol/mol of VAc) and low reaction temperatures were employed, the conversion increased steadily up to 85-95%, depending on the MMT content in the system. The effect of initiator concentration on the polymerization rate is shown in Figure 5(c). It can be seen that the polymerization rate, at a reaction temperature of 30 °C, increased with the increasing initiator concentrations, in accordance with theoretical prediction (Odian, 1981).

2.2.2.2 Morphology and structure property

SEM photographs of pure PVAc and PVAc/MMT nanocomposite microspheres with 1 wt.% MMT contents are presented in Figure 6. As expected, the surface of pure PVAc microparticles shown in Figure 6(a) is smooth. Figure 6(b) shows that the roughness of the microsphere surface is increased by adding the MMT. To further study the distribution of MMT particles in the PVAc microspheres, the fracture surfaces of the PVAc/MMT nanocomposite microparticles were investigated. Although it is not shown here, MMT particles were embedded inside the composite microspheres, which indicate that PVAc/MMT microspheres could be prepared by *in-situ* suspension polymerization.

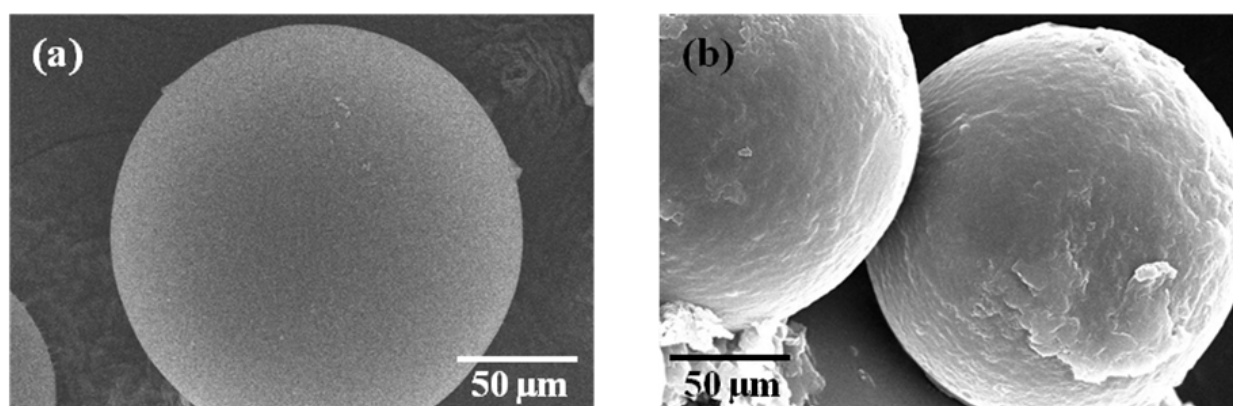


Fig. 6. SEM images of (a) pure PVAc microparticles and (b) PVAc/MMT nanocomposite microparticles with MMT concentration of 1 wt. %

The detail structure of the clay nanocomposites has been established using XRD analysis. Figure 7 shows the XRD patterns of the PVAc, MMT, and PVAc/MMT with MMT content of 1 wt.%. The MMT shows a diffraction pattern peak at $2\theta = 7.2^\circ$, which corresponds to the average basal spacing (d-spacing) of 12.3 Å. In the PVAc/MMT nanocomposite microparticles, the peak moved to a lower angle, i.e., $2\theta = 2.7^\circ$. The basal spacing increased from 12.3 to 32.6 Å. This spacing indicates that long alkyl (cetyltrimethyl) ammonium ions were inserted into the gallery of MMT; as a result, an intercalated structure formed. The inserted long alkyl chains caused the hydrophilic nature of the clay to decrease, and this effect improved the dispersion of silicates in the polymer matrix.

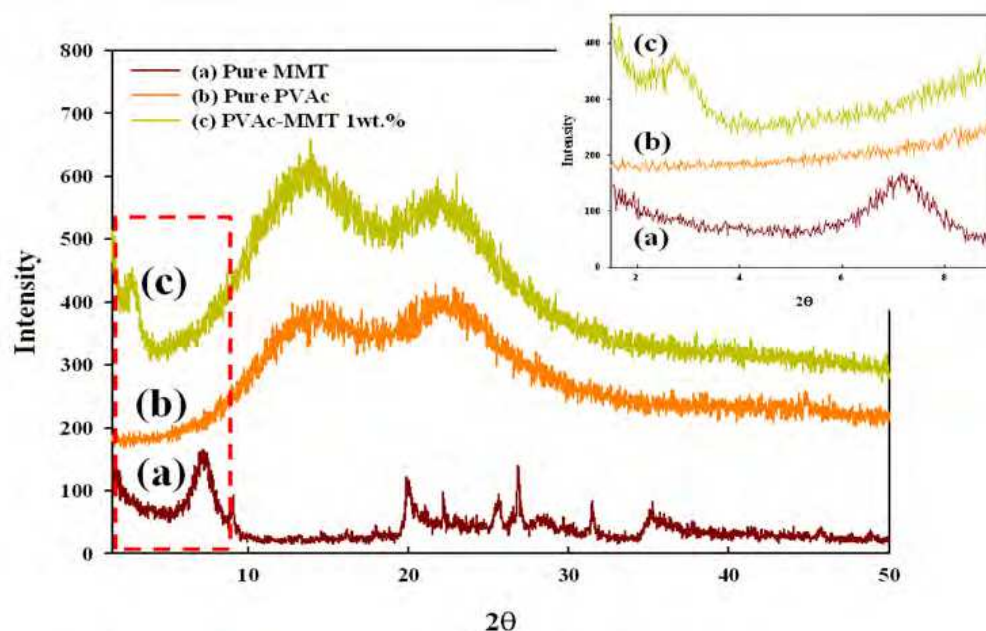


Fig. 7. XRD patterns of (a) pure PVAc microparticles, (b) pure MMT, and (c) PVAc/MMT nanocomposite microparticles with MMT concentration of 1 wt.%

2.2.2.3 Heterogeneous saponification of PVAc/MMT microparticles

The PVA obtained by the saponification of poly(vinyl ester) is a linear semicrystalline polymer and has been widely used as fibers for textile industries, films, membranes, and drug delivery systems. In this study, the PVA/MMT nanocomposite microspheres were prepared by a simple heterogeneous saponification method. To preserve the spherical shapes of PVAc/MMT nanocomposite particles, the saponification was carried out by disperse PVAc/MMT nanocomposite particles in alkali aqueous solution with very gentle agitation. The effect of MMT on the PVAc saponification rate was recorded by optical microscope observation. In this study, the heterogeneous saponifications of pure PVAc and PVAc/MMT microspheres were conducted under the same conditions. Degree of saponification (DS) is defined by the volume ratio of PVAc/PVA.

Figure 8 shows the optical micrographs of PVAc/PVA (Figure 8a,b) and PVA/PVAc/MMT (Fig. 8. c,d) nanocomposite microspheres prepared by heterogeneous saponification at different reaction times. As shown in Figure 8c,d, partially saponified nanocomposite microparticles (MMT content of 1 wt.%, degrees of saponification are 18.2 and 51.3%, respectively) with a PVAc core and PVA shell structure could be obtained by controlling the saponification degrees. It can be seen that the MMT presented in the PVAc microparticles

significantly increase the DS of PVAc. It is well known that MMT is high swollable in alkaline solution, which results in a faster diffusion of base molecules into the PVAc particles to accelerate the saponification rate of the PVAc microparticles. Figure 9 shows the effect of MMT contents on the DS of PVAc microparticles, which indicates that the saponification rate increased remarkably with increasing MMT addition.

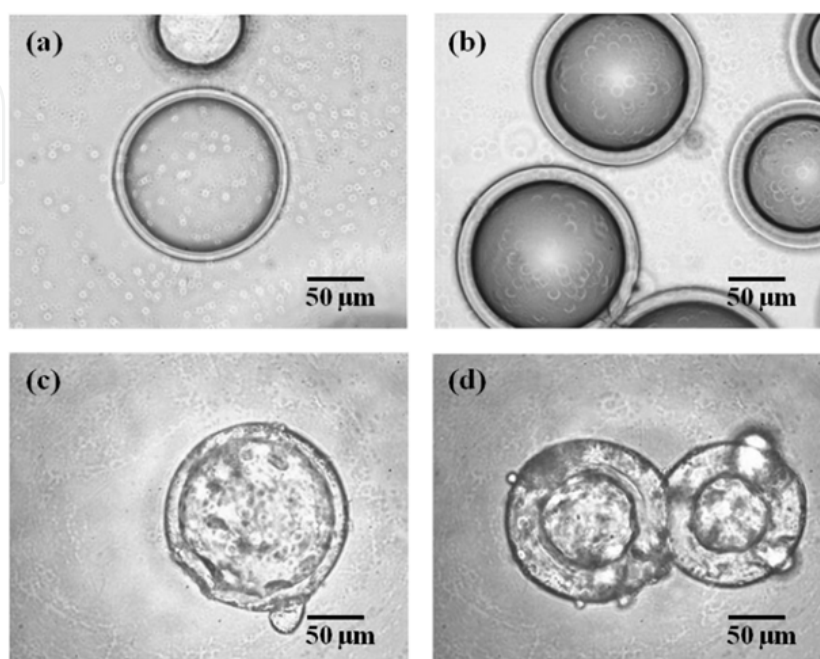


Fig. 8. Optical micrographs of (a,b) PVAc/PVA nanocomposite microparticles and (c, d) PVA/PVAc/MMT nanocomposite microparticles with MMT concentration of 1 wt.%. The saponification times and DS values were (a) 2 h and 14.7%, (b) 4 h and 17.5%, (c) 2 h and 18.2%, and (d) 4 h and 51.3%

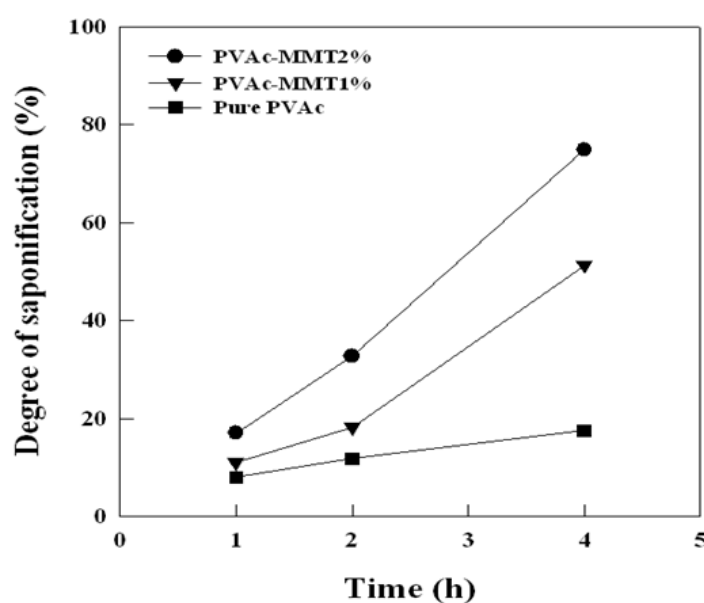


Fig. 9. Effect of MMT contents on the DS of PVAc/PVA microparticles with saponification time

The structures of the PVAc/MMT and PVA/PVAc/MMT nanocomposite microparticles were analyzed by using FT-IR spectroscopy. Figure 10 shows the FT-IR spectra for (A) pure MMT, pure PVAc microspheres, PVAc/MMT nanocomposite microparticles with MMT content of 1 wt.%, and (B) saponified PVA/PVAc/MMT nanocomposite microparticles. It is well known that pure MMT shows three strong peaks at 455, 520, and 1045 cm^{-1} . These peaks are associated with the bending mode of Si-O, the stretching vibration of Al-O, and the stretching vibration of Si-O, respectively. One can easily see peaks of both PVAc and MMT component in the spectrum of PVAc/MMT nanocomposite microparticles. It should be noted that MMT incorporated polymer particles could be prepared by the in situ suspension polymerization of VAc in the presence of organophilic MMT nanoparticles. From the generation of the -OH stretching vibration in the region of 3000-3600 cm^{-1} after the saponification process Figure 10(B), it is obvious that the surfaces of the PVAc/MMT nanocomposite microparticles were saponified with the hydroxyl groups.

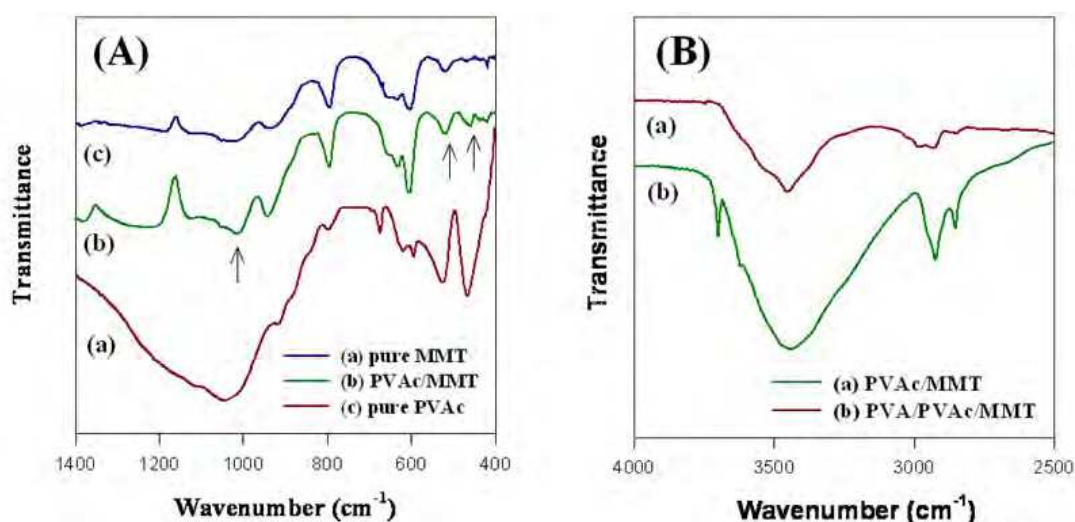


Fig. 10. FT-IR spectra of (A) pure MMT, pure PVAc microspheres, PVAc/MMT nanocomposite microparticles and (B) PVAc/MMT, PVA/PVAc/MMT nanocomposite microparticles (MMT concentration of 1 wt.%)

3. Fabrication and characterization of several types of polymer nanocomposite particles by one step electro spraying technique

The great advantage offered by electro spraying than other commonly used are simplicity and possibility for continuous one step process. The principle of electro spraying is same as electro spinning. High voltage is applied to a polymer fluid such that charges are induced within the fluid. When charges within the fluid reached a critical amount, a fluid jet will erupt from the droplet at the tip of the needle resulting in the formation of a Taylor cone. The electro spraying jet will travel towards the region of lower potential, which in most cases, is a grounded collector. The most important variable distinguishing electro spraying and electro spinning is solution parameter such as polymer molecular weight, concentration and viscosity, etc..

The major purpose of this section is to design an optimum solution parameter for electro spraying system and evaluate inorganic material effects such as antibacterial performance and thermal properties. PVA, PVA/MMT, PVA/Ag, and PVA/MMT/Ag

nanocomposite nanoparticles which have an average diameter about 350 nm are successfully fabricated by one step electro spraying process in aqueous solution (Park et al., 2011; Park et al., 2011). In order to investigate the effect of MMT and Ag on the morphology, size, physical properties and anti-bacterial efficacy of composites, experiments were performed varying MMT and Ag concentrations. Transmission electron microscopy and reflection type X-ray diffraction analysis shows MMT and Ag were well dispersed in PVA nanoparticles. Those inorganic nanoparticles simultaneously enhanced thermal properties and anti-bacterial performance of the composite materials. The results obtained in this study may help to fabricate nanocomposite nanoparticle by one step process that can be utilized in biomedical application such as drug delivery system and functional nanoparticle for diagnosis and treatment.

3.1 Experimental

3.1.1 Materials

PVA with $P_n = 500$ (low-molecular-weight LMW) and 1700 (medium-molecular-weight, MMW) [fully hydrolyzed, degree of saponification = 99.9%] was obtained from DC Chemical Co., Seoul, Korea and MMT was purchased from Kunimine Industries Co., Japan. Aqueous silver nanoparticle dispersion (AGS-WP001, 10,000 ppm) with diameters ca.15-30 nm was got from Miji Tech., Korea. Doubly distilled water was used as a solvent to prepare all solutions.

3.1.2 Preparation of electro spraying solution

At first, 5 wt.% MMT powder was dispersed in distilled water under magnetic stirring for 1 h at room temperature. After making MMT dispersion, various concentrations of both LMW and MMW type of PVA were added in that solution. The solution was heated in a water bath at 80 °C under magnetic stirring for 2 h followed by cooling to room temperature. The PVA/MMT/Ag solution was made ready by mixing of PVA/MMT solution and Ag nanoparticles dispersion with different concentrations of Ag (1 and 3 wt.%) by stirring for more 2h at room temperature. The content of 5 wt.% of MMT in PVA nanocomposite nanofiber revealed best properties in our previous report (Ji et al., 2009; Lee et al., 2009; Park et al., 2009) which was predominant reason for using same concentration of MMT in this experiment.

Condition	Type of nanoparticles				
	LMW-PVA	MMW-PVA	PVA/MMT	PVA/Ag	PVA/MMT/Ag
Polymer concentration	2.5, 5, 7.5, 10 wt.%	2.5, 5, 7.5, 10 wt.%	2.5 wt.% of LMW PVA	2.5 wt.% of LMW PVA	2.5 wt.% of LMW PVA
MMT concentration*	-	-	5 wt. %	-	5 wt. %
Ag concentration*	-	-	-	1, 3 wt. %	1, 3 wt. %
Voltage	15 kV				
Tip collector distance	15 cm				

* based on polymer concentration

Table 2. Electro spraying condition of PVA/MMT/Ag nanocomposite nanoparticles

3.1.3 Electrospaying

During electrospaying, a high voltage power (CHUNGPA EMT Co., Ltd., Seoul, Korea; model CPS-60K02VIT) was applied to the electrospaying solution contained in a syringe via an alligator clip attached to the syringe needle. The applied voltage was adjusted at 15 kV. The solution was delivered to the blunt needle tip via syringe pump to control the solution flow rate. When a high electric field is applied to the solution in the syringe, droplets form at the nozzle tip in the form of a cone called Taylor cone. Eventually electrical forces overcome the surface tension of the solution, and a straight jet ejects from the apex of the cone. This jet breaks up into particles while traveling towards a grounded collector placed at 15 cm vertical distance to the needle tip due to inherent instabilities generated by the electric field. Particles were collected on an electrically grounded aluminum foil placed at 15 cm vertical distance to the needle tip.

3.1.4 Preservation test

The preservation efficacy of the nanocomposite nanoparticles was tested to evaluate the antimicrobial property. Samples were prepared by dispersing the nanoparticles in a viscous aqueous solution containing 0.01 wt.% of neutralized polyacrylic acid (Carbopol 941, Noveon Inc.). A mixed culture of microorganisms, *Staphylococcus aureus* (ATCC6538), and *Escherichia coli* (ATCC25922) were obtained on tryptone soya broth after 24h incubation at 32 °C. Then, 20 g of samples were inoculated with 0.2 g of the microorganism suspensions to adjust the initial concentration of bacteria to 10⁷ cfu/g. Then, the inoculants were mixed homogeneously with the samples and stored at 32 °C. The microbial counts were carried out using the pour plate count method.

3.1.5 Characterizations

The morphology and structure of nanocomposite nanoparticles were observed with FE-SEM after gold coating and TEM analysis. XRD was used the Cu K α radiation with wavelength of 0.154 nm. The scanning rate was 2°/min ranging 2 to 50° (2 θ). The thermal behavior of nanocomposite nanoparticles was studied with TGA techniques (model Q-50) from TA instruments, USA at the rate of 10 °C/min from room temperature to 600 °C under the nitrogen gas atmosphere. The antibacterial performance was investigated to examine the biological function of PVA/MMT/Ag nanocomposite nanoparticles by KSM 0146 (Shake flask method) using *Staphylococcus aureus* and *Escherichia coli*.

3.2 Results and discussion

3.2.1 Effect of molecular weight and concentration

The nanoparticle formation conditions are strictly dependent on the polymer molecular weight and concentration. Nanoparticles could be obtained when either the molecular weight of the polymer and concentration of the polymer solution were too low and when it was used as the precursor in the electrospaying process. To the contrary, cone jet of polymer solution with sufficient resistance to shear stress will not break up to form them after solvent evaporation by a process called electrospinning (Li et al., 2004). Also, it must be considered that, when working in the electrospaying, the usual shape of the forming spherical particles is due to the physical properties of the system (Rayleigh et al., 1882).

To obtain the nanoparticles, a series of experiments with different solution concentrations of LMW-PVA (2.5 to 15 wt %) were conducted, and the results are presented in Figures 11 and 12. From Figures 11 and 12, it is clearly evident that nanoparticles are formed in case of

2.5 wt. % of LMW-PVA concentration. Polymer concentration above 2.5 wt. %, particles exhibit a spindle shape with one or two tail and fibrous shape. The polymers with higher molecular weight tended to attain a highly elongated shape like fibrous structure easily than low molecular weight polymer.

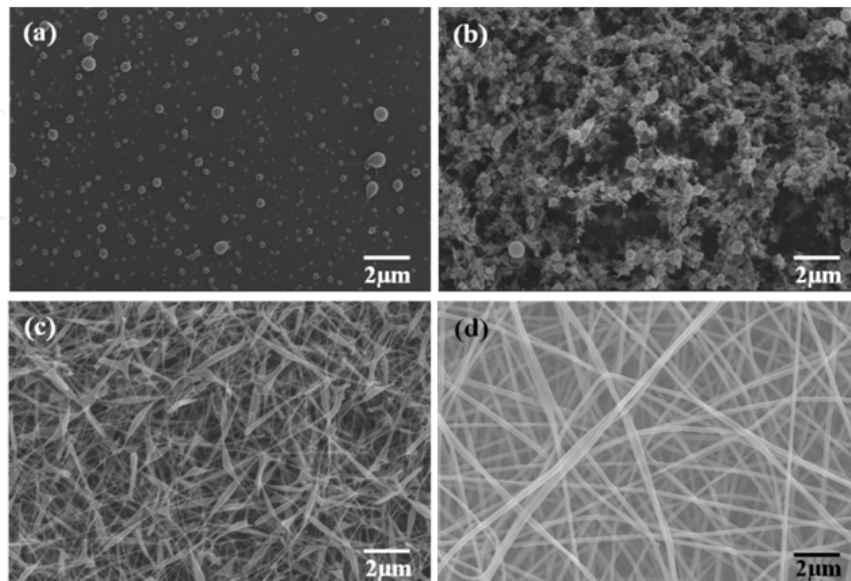


Fig. 11. FE-SEM images of LMW-PVA nanostructure syntheses by using different concentration of (a) 2.5 wt.%, (b) 5 wt.%, (c) 10 wt.% and (d) 15 wt.% (TCD= 15 cm and applied voltage= 15 kV; inset: high magnification morphologies of related images)

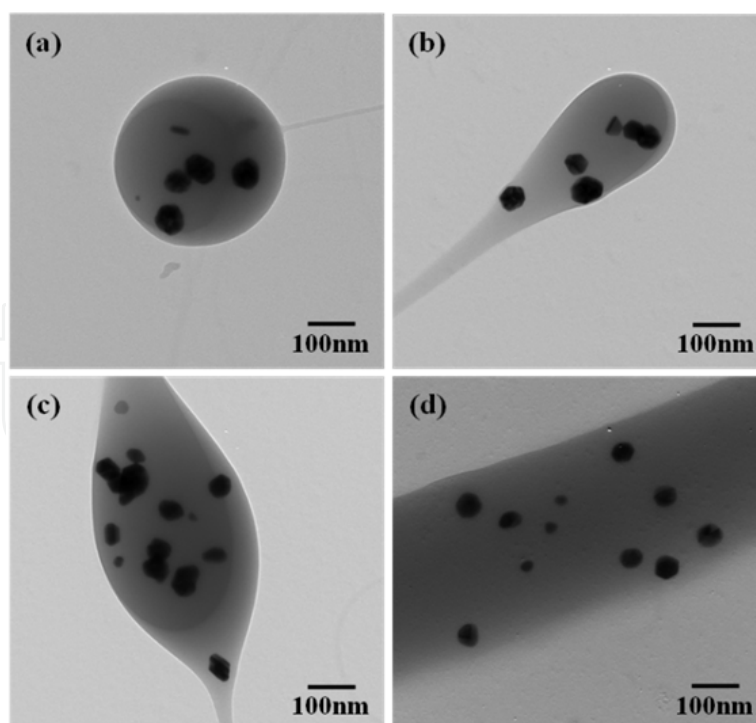


Fig. 12. TEM images of LMW-PVA/Ag nanostructure syntheses by using different concentration of PVA (a) 2.5 wt.%, (b) 5 wt.%, (c) 7.5 wt.% and (d) 15 wt.% (TCD= 15 cm and applied voltage= 15 kV and Ag concentration= 1 wt.%)

It is suggested that increasing entanglement of polymer chains caused highly by molecular weight and polymer concentration that contribute to the formation of the fibrous structure. Actually, MMW-PVA formed not only nanoparticle but also just bring forth spindle like shape at low concentration. On the contrary, in case of LMW-PVA, spherical nanoparticles were formed at 2.5 wt.% of polymer concentration. Another concentration of LMW-PVA showed more beaded morphology than MMW-PVA due to the low molecular weight and low viscosity of the spraying solution. The reason for different shape at each concentration is the Raleigh forces, which assist in particle formation, are able to overcome the viscous forces to enable the formation of spherical particles (Shin et al., 2001). Particles, which are obtained from PVA concentration above 2.5 wt.%, exhibit a spindle shape with one or two tail and fiber shape.

3.2.2 Morphology and structure

Successful formation of the PVA/MMT/Ag nanocomposite nanoparticles are illustrated by TEM images (Figure 13). The pure polymer nanoparticles were generally spherical with smooth surfaces at 2.5 wt.% concentration of LMW-PVA. The mean size of nanoparticles varied between 300 to 450 nm depending on the process parameter. When MMT clay was added, the nanoparticle morphology and shape are dramatically changed from sphere to rugged particle. TEM images support that the coexistence of Ag nanoparticles and PVA matrix for LMW-PVA/Ag nanocomposite nanoparticles. Small dark dots indicate the Ag nanoparticles which are seen from TEM images in nanocomposite nanoparticles. Due to the strong interactions between polymer and metal, Ag nanoparticles are well embedded in the PVA matrix. Also, it can be clearly observed that each silicate platelet forms a dark line in the

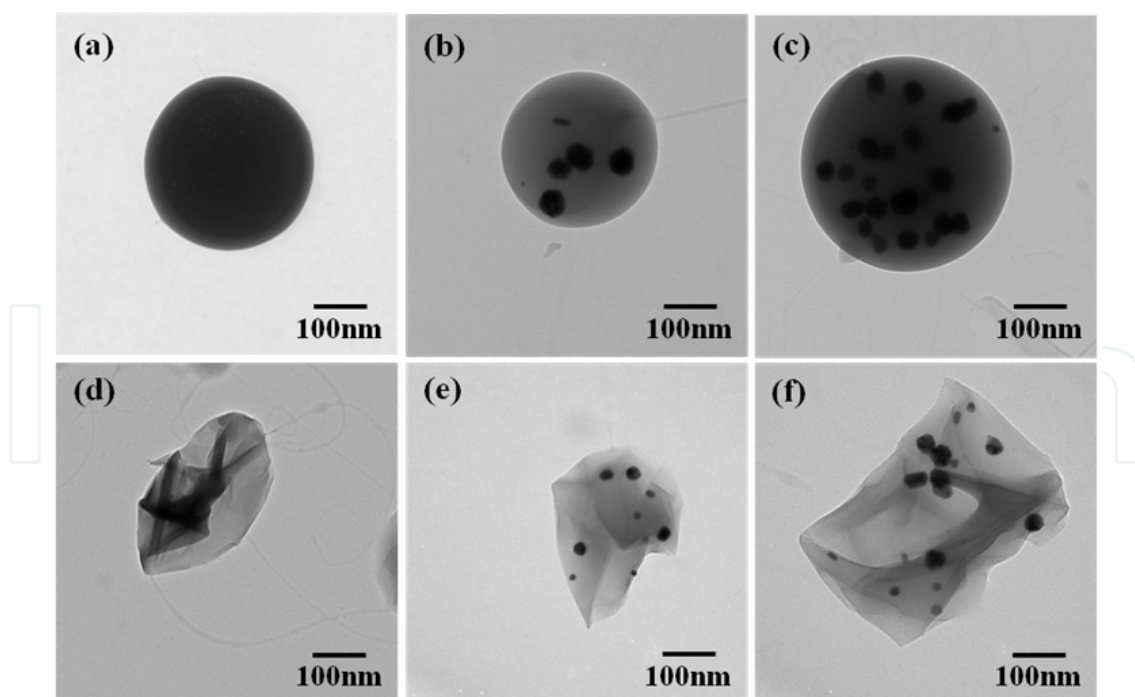


Fig. 13. TEM images of (a) PVA nanoparticles, (b) PVA/Ag 1wt.%, (c) PVA/Ag 3wt.%, (d) PVA/MMT (e) PVA/MMT/Ag 1wt.%, and (f) PVA/MMT/Ag 3wt.% nanocomposite nanoparticles (LMW-PVA solution concentration= 2.5 wt.%, MMT concentration= 5 wt.%, TCD= 15 cm and applied voltage= 15 kV)

nanoparticle compare with the pure PVA spherical nanoparticle. The size of the dark line is about 1–3 nm in width and 100–200 nm in length, and it indicated the good dispersion and exfoliation of MMT layers in the nanoparticle. Well-dispersed Ag and MMT were shown in Figure 13 from where we can see Ag and MMT were dispersed inside the polymer matrix without agglomeration. TEM results reveal that the MMT and Ag are distributed uniformly in the PVA/MMT/Ag nanocomposite nanoparticles.

The XRD patterns of nanocomposite nanoparticles show three diffraction peaks at 2θ of ca. 19.3° , 38.2° and 44.6° (Figure 14). The pure PVA shows a significant crystalline peak at about 19.3° , which is because of the occurrence of string inter- and intramolecular hydrogen bonding (Figure 14a). In case of clay-polymer composite, unexfoliated or intercalated MMT usually shows a peak in the range $3\sim 9^\circ$ (2θ). In exfoliated nanocomposites, generally single silicate layers (1–3 nm thick) are homogeneously dispersed in the polymer matrix, and XRD pattern with no distinct diffraction peak in the range of $3\sim 9^\circ$ (2θ) could be observed. The peaks of silver particles become gradually enlarged with increasing the content of Ag nanoparticles and crystallinity of PVA/MMT ($2\theta = 19.3^\circ$) is lower in comparison with Figure 14(a) and (b). These peaks are corresponding to the (111) and (200) planes of the silver nanocrystals with cubic symmetry. XRD results indicate that MMT and Ag particles are well dispersed in the PVA matrix and MMT is predominantly exfoliated. Moreover, TEM images confirm MMT and Ag nanoparticles in the PVA/MMT/Ag hybrid nanoparticles (Figure 13).

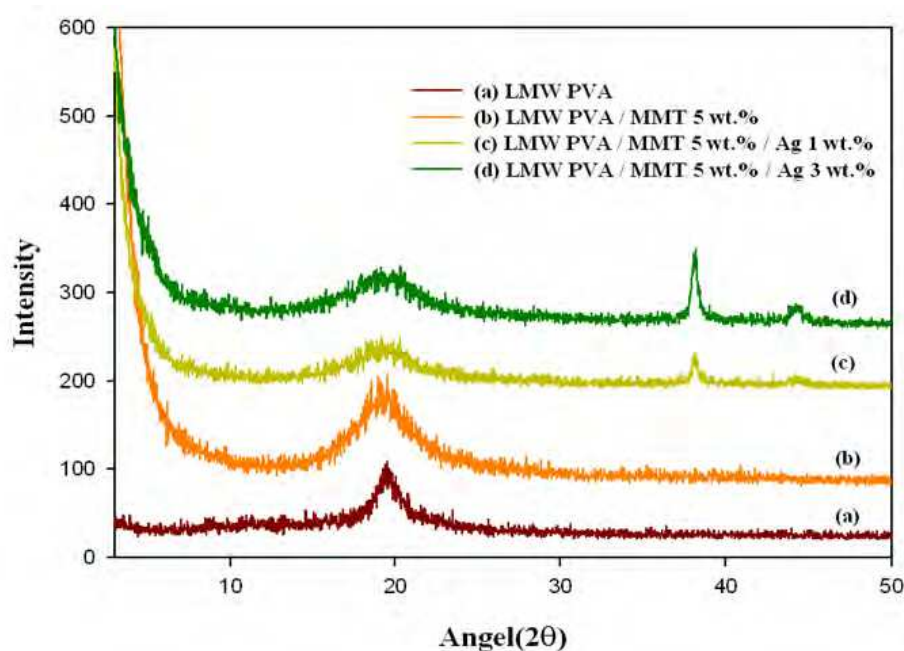


Fig. 14. XRD data of (a) PVA nanoparticles, (b) PVA/MMT nanocomposite nanoparticles, and PVA/MMT/Ag nanocomposite nanoparticles prepared with different Ag contents of (c) 1 wt.%, (d) 3 wt.% (LMW-PVA solution concentration= 2.5%, MMT concentration= 5 wt.%)

3.2.3 Thermal stability

Thermal stability of nanocomposite nanoparticles was measured using TGA in nitrogen atmosphere. The actual decomposition temperature depends on the structure, molecular weight and conformation of the polymer. Typical three weight loss peaks were observed in

the TGA curve for bulk PVA. The first peak at 50-70 °C was due to its moisture vaporization, the second peak at 260-380 °C was due to the thermal degradation of PVA, and the third peak at 430-460 °C was due to the byproduct formation of PVA during the TGA thermal degradation process. Figure 15 shows TGA thermograms of different decomposition temperature with Ag contents of 0, 1 and 3 wt.%. Within up to 225 °C, there is an increased in thermal stability from the pure LMW-PVA nanoparticle to PVA/MMT/Ag nanocomposite nanoparticles. The higher thermal stability might be attributed due to its higher contents of Ag nanoparticles in the PVA/MMT/Ag nanocomposite nanoparticles.

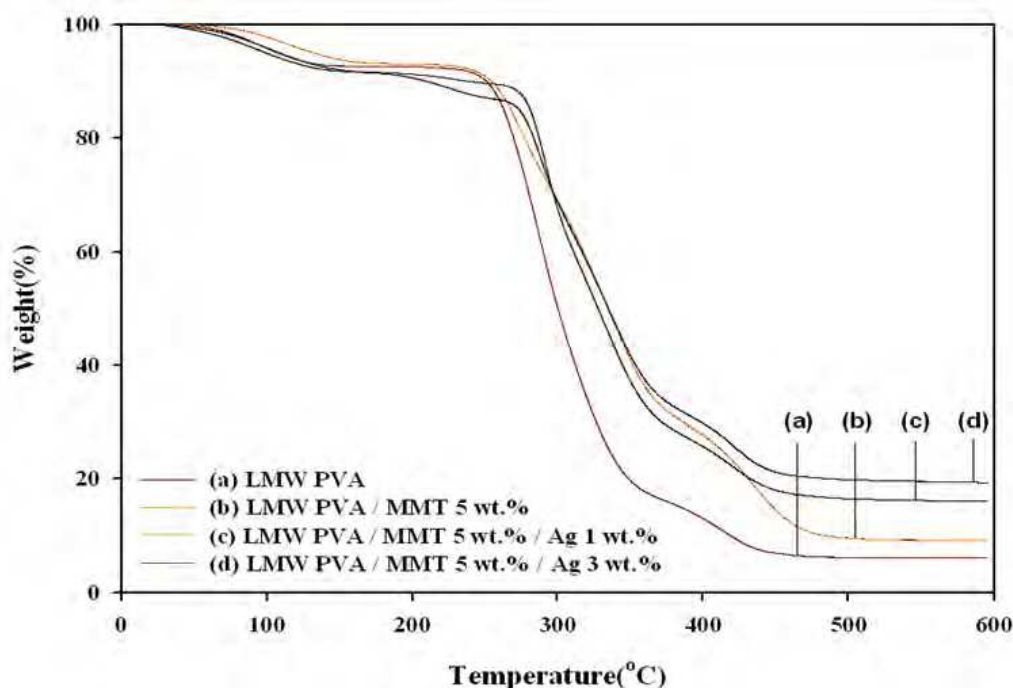


Fig. 15. TGA data of (a) LMW-PVA nanoparticle, (b) PVA/MMT nanocomposite nanoparticles, and PVA/MMT/Ag nanocomposite nanoparticles prepared with different Ag contents of (c) 1 wt.%, (d) 3 wt.% (LMW-PVA solution concentration= 2.5%, MMT concentration= 5 wt.%)

3.2.4 Anti-bacterial efficacy

Ag nanoparticles have been known to have strong inhibitory and antibacterial effects as well as a broad spectrum of antimicrobial activities (Dowling et al., 2001). In this study, in order to provide useful information for the biological function of PVA/MMT/Ag nanocomposite nanoparticles, the anti-bacterial performance of PVA/MMT/Ag nanocomposite nanoparticles were evaluated in viscous aqueous test samples and shown in Figure 16. The antibacterial activity of PVA/MMT/Ag nanocomposite nanoparticle is assessed by counting the number of bacteria in the sample with the storage time at 32 °C. As shown in Figure 16, in the absence of Ag nanoparticles, the number of bacteria remained constant. However, after adding Ag nanoparticles into the nanoparticles, all of bacteria decreased dramatically.

The increase in the concentration of the Ag accelerates diminishing in bacteria. With only a small amount of Ag, almost all the initially inoculated bacteria could be sterilized within a week.

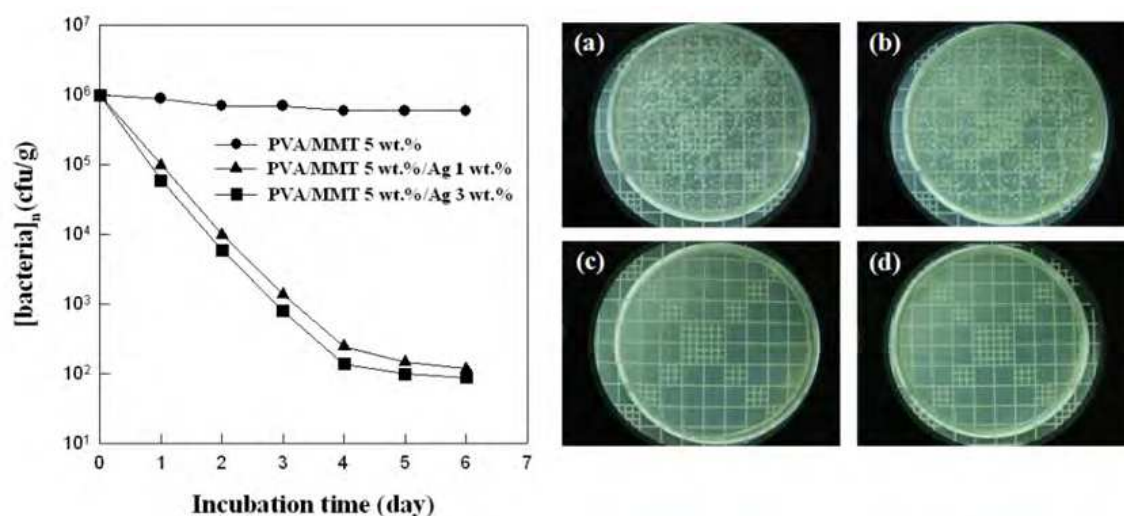


Fig. 16. Antibacterial ability test with *Staphylococcus aureus* (a) control and PVA/MMT/Ag hybrid nanoparticles containing with different Ag amounts of (b) 0 wt. %, (c) 1 wt.%, and (d) 3 wt.% (after 1week)

3.2.5 Application of polymer/natural extracts nanoparticles for children's products

Based on the above results, we prepared polymer/natural colorant nanoparticles for using children's products. Excellent antibacterial ability of the PVA/MMT/Ag nanocomposite nanoparticles has been proven, so polymer nanocomposite nanoparticles containing natural colorant, Cyanidin-3-O-glucoside, extracted from sorghum, has advantage of safety for using children's products over existing compound materials. Figure 17 is chemical structure of Cyanidin-3-O-glucoside and Figure 18 shows TEM image of prepared polymer nanocomposite nanoparticles containing Cyanidin-3-O-glucoside.

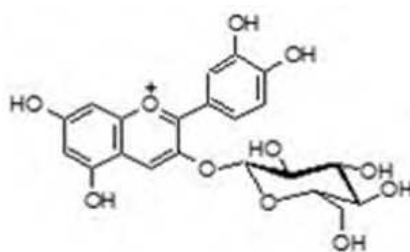


Fig. 17. Chemical structure of Cyanidin-3-O-glucoside

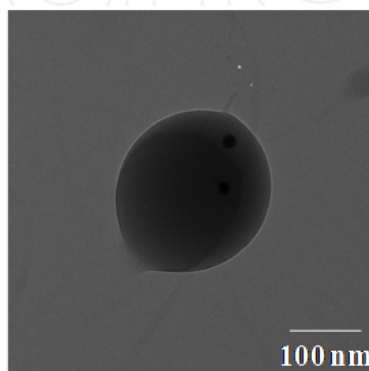


Fig. 18. TEM image of polymer/Cyanidin-3-O-glucoside nanoparticle

4. Conclusion

In this work, PVAc/Ag and PVA/PVAc/MMT nanocomposite microparticles were prepared by low temperature *in-situ* suspension polymerization of VAc in the presence of Ag and MMT and PVA/MMT, PVA/MMT/Ag nanocomposite nanoparticles are successfully fabricated from aqueous solutions by one step electro spraying technique. The morphology of PVAc/Ag nanocomposite microparticles was influenced by surfactant. By a heterogeneous saponification method, PVA/PVAc/MMT nanocomposite microparticles with core/shell structure could be prepared. Morphology of nanocomposite nanoparticles prepared by electro spraying technique can be affected by the molecular weight of polymer and concentration of polymer solution. The thermal properties of prepared nanocomposite micro- and nanoparticles enhanced with the addition of MMT and Ag. Moreover, it has good anti-bacterial performance. The results obtained in this study may help to fabricate various type of nanocomposite micro- and nanoparticle by *in-situ* polymerization and one step process that can be utilized in not only biomedical application such as drug delivery system and functional nanoparticle for diagnosis and treatment, but bioaffinity materials like children and food industries.

5. Acknowledgements

This research was financially supported in part by grants from the Agenda Program (PJ0073852010) of National Institute of Crop Science, Rural Development Administration (RDA), Korea. Also, this research was partially supported by a grant(70011324) from Daegu Technology Development Program of the Daegu Regional Government.

6. References

- Berkland, C.; Kim, C. & Pack, D.W. (2001). Fabrication of PLG microspheres with precisely controlled and monodisperse size distributions. *J. Control. Release*, 73, 1, 59-74, 0168-3659
- Dong, A.G.; Wang, Y.J. & Tang, Y. (2002). Fabrication of compact silver nanoshells on polystyrene spheres through electrostatic attraction. *Chem. Commun.*, 4, 350-351, 1359-7345
- Dowling, D.P.; Donnelly, K.; McConnell, M.L.; Eloy, R. & Arnaud, M.N. (2001). Deposition of anti-bacterial silver coatings on polymeric substrates. *Thin Solid Films*, 398-399, 602-606, 0040-6090
- Giannetti, E. & Mazzocchi, R. (1986). High conversion free-radical suspension polymerization: End groups in poly(methyl methacrylate) and their influence on the thermal stability. *J. Polym. Sci. Pol. Chem.*, 24, 10, 2517-2551, 0087-624X
- Gotoh, Y.; Igarashi, R.; Ohkoshi, Y.; Nagura, M.; Akamatsu, K. & Deki, S. (2000). Preparation and structure of copper nanoparticle/poly(acrylic acid) composite films. *J. Mater.Chem.*, 10, 11, 2548-2552, 0959-9428
- Hatchett, D.W.; Josowicz, M.; Janata, J. & Baer, D.R. (1999). Electrochemical formation of Au clusters in polyaniline. *Chem. Mater.*, 11, 10, 2989-2994, 0897-4756
- Huang, C.J.; Yen, C.C. & Chang, T.C. (1991). Studies on the preparation and properties of conductive polymers. III. Metallized polymer films by retroplating out. *J. Appl. Polym. Sci.*, 42, 8, 2237-2245, 0021-8995

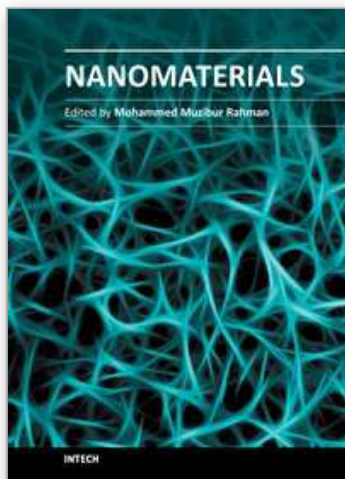
- Ji, H.M.; Lee, H.W.; Karim, M.R.; Cheong, I.W.; Bae, E.A.; Kim, T.H.; Islam, M.S.; Ji, B.C. & Yeum, J.H. (2009). Electrospinning and characterization of medium-molecular-weight poly(vinyl alcohol)/high-molecular-weight poly(vinyl alcohol)/montmorillonite nanofibers. *Colloid Polym. Sci.*, 287, 7, 751-758, 0303-402X
- Jung, H.M.; Lee, E.M.; Ji, B.C.; Deng, Y.; Yun, J.D. & Yeum, J.H. (2007). Poly(vinyl acetate)/poly(vinyl alcohol)/montmorillonite nanocomposite microspheres prepared by suspension polymerization and saponification. *Colloid Polym. Sci.*, 285, 6, 705-710, 0303-402X
- Jung, H.M.; Lee, E.M.; Ji, B.C.; Sohn, S.O.; Ghim, H.D.; Cho, H.; Han, Y.A.; Choi, J.H.; Yun, J.D. & Yeum, J.H. (2006). Preparation of poly(vinyl acetate)/clay and poly(vinyl acetate)/poly(vinyl alcohol)/clay microspheres. *Fiber. Polym.*, 7, 3, 229-234, 1229-9197
- Lee, E.M.; Lee, H.W.; Park, J.H.; Han, Y.A.; Ji, B.C.; Oh, W.; Deng, Y. & Yeum, J.H. (2008). Multihollow structured poly(methyl methacrylate)/silver nanocomposite microspheres prepared by suspension polymerization in the presence of dual dispersion agents. *Colloid Polym. Sci.*, 286, 12, 1379-1385, 0303-402X
- Lee, H.W.; Karim, M.R.; Ji, H.M.; Choi, J.H.; Ghim, H.D.; Park, J.H.; Oh, W. & Yeum, J.H. (2009). Electrospinning fabrication and characterization of poly(vinyl alcohol)/montmorillonite nanofiber mats. *J. Appl. Polym. Sci.*, 113, 3, 1860-1867, 0021-8995
- Lee, J.E.; Kim, J.W.; Jun, J.B.; Ryu, J.H.; Kang, H.H.; Oh, S.G. & Suh, K.D. (2004). Polymer/Ag composite microspheres produced by water-in-oil-in-water emulsion polymerization and their application for a preservative. *Colloid Polym. Sci.*, 282, 3, 295-299, 0303-402X
- Li, D. & Xia, Y.N. (2004). Electrospinning of nanofibers: Reinventing the wheel?. *Adv. Mater.*, 16, 14, 1151-1170, 0935-9648
- Ma, G.; Nagai, M. & Omi, S. (1999). Preparation of uniform poly(lactide) microspheres by employing SPG emulsification technique. *Colloid Surface. A*, 153, 1-3, 383-394, 0927-7757
- Matsumoto, H.; Mizukoshi, T.; Nitta, K.; Minagawa, M.; Tanoika, A. & Yamagata, Y. (2005). Organic/inorganic hybrid nano-microstructured coatings on insulated substrates by electrospray deposition. *J. Colloid Interf. Sci.*, 286, 1, 414-416, 0021-9797
- Messersmith, P.B. & Giannelis, E.P. (1993). Polymer-layered silicate nanocomposites: In situ intercalative polymerization of ϵ -caprolactone in layered silicates. *Chem. Mater.*, 5, 8, 1064-1066, 0897-4756
- Mu, L. & Feng, S.S. (2001). Fabrication, characterization and in vitro release of paclitaxel (Taxol®) loaded poly(lactic-co-glycolic acid) microspheres prepared by spray drying technique with lipid/cholesterol emulsifiers. *J. Control. Release*, 76, 3, 239-254, 0168-3659
- Odian, G. (1981). Principles of polymerization. 2nd edn. *John Wiley & Sons, Inc.*,
- Okamoto, M.; Morita, S.; Taguchi, H.; Kim, Y.H.; Kotaka, T. & Tateyama, H. (2000). Synthesis and structure of smectic clay/poly(methyl methacrylate) and

- clay/polystyrene nanocomposites via in situ intercalative polymerization. *Polymer*, 41, 10, 3887-3890, 0032-3861
- Okuda, H. & Kelly, A.J. (1996). Electrostatic atomization—experiment, theory and industrial applications. *Phys. Plasmas*, 3, 5, 2191-2196, 1070-664X
- Oriakhi, C.O. & Lerner, M.M. (1995). Poly(pyrrole) and poly(thiophene)/clay nanocomposites via latex-colloid interaction. *Mater. Res. Bull.*, 30, 6, 723-729, 0025-5408
- Park, J.H.; Kim, I.K.; Oh, W.; Deng, Y.; Kim, J.W. & Yeum, J.H. Electro spraying fabrication and characterization of low molecular weight poly(vinyl alcohol)/silver composite nanospheres for antibacterial applications. *Polym. Polym. Compos., in Press*, 0967-3911
- Park, J.H.; Lee, H.W.; Chae, D.K.; Oh, W.; Yun, J.D.; Deng, W. & Yeum, J.H. (2009). Electro spinning and characterization of poly(vinyl alcohol)/chitosan oligosaccharide/clay nanocomposite nanofibers in aqueous solutions. *Colloid Polym. Sci.*, 287, 8, 943- 950, 0303-402
- Park, S.M.; Park, J.H.; Islam, M.S.; Choi, J.H.; Yoon, N.S. & Yeum, J.H. (2011). Preparation of low molecular weight poly(vinyl alcohol)/montmorillonite composite nanoparticles using electro spraying technique. *Polym. Polym. Compos.*, 19, 1, 1-6, 0967-3911
- Ramos, J.; Millan, A. & Palacio, F. (2000). Production of magnetic nanoparticles in a polyvinylpyridine matrix. *Polymer*, 41, 24, 8461- 8464, 0032-3861
- Rayleigh, L. (1882). On the equilibrium of liquid conducting masses charged with electricity. *Philos. Mag.*, 14, 87, 184-186, 1478-6435
- Rosca, I.D.; Watari, F. & Uo, M. (2004). Microparticle formation and its mechanism in single and double emulsion solvent evaporation. *J. Control. Release*, 99, 2, 271-280, 0168-3659
- Salata, O.V.; Hull, P.J. & Dobson, P.J. (1997). Synthesis of nanometer-scale silver crystallites via a room-temperature electrostatic spraying process. *Adv. Mater.*, 9, 5, 413-417, 0935-9648
- Shin, Y.M.; Hohman, M.M.; Brenner, M.P. & Rutledge, G.C. (2001). Electro spinning: A whipping fluid jet generates submicron polymer fibers. *Appl. Phys. Lett.*, 78, 8, 1149-1151, 0003-6951
- Sinha, V.R.; Bansal, K.; Kaushik, R. & Trehan, A. (2004). Poly- ϵ -caprolactone microspheres and nanospheres: an overview. *Int. J. Pharmaceut.*, 278, 1, 1-23, 0378-5173
- Usuki, A.; Kojima, Y.; Kawasumi, M.; Okada, A.; Fukushima, Y.; Kurauchi, T. & Kamigaito, O. (1993). Synthesis of nylon 6-clay hybrid. *J. Mater. Res.*, 8, 5, 1179-1184, 0884-2914
- Wu, W.; He, T. & Chen, J.F. (2006). Study on in situ preparation of nano calcium carbonate/PMMA composite particles. *Mater. Lett.*, 60, 19, 2410-2415, 0167-577X
- Yeum, J.H. & Deng, Y. (2005). Synthesis of high molecular weight poly(methyl methacrylate) microspheres by suspension polymerization in the presence of silver nanoparticles. *Colloid Polym. Sci.*, 283, 11, 1172-1179, 0303-402X

- Yeum, J.H.; Qunhui, S. & Deng, Y. (2005). Poly(vinyl acetate)/silver nanocomposite microspheres prepared by suspension polymerization at low temperature. *Macromol. Mater. Eng.*, 290, 1, 78-84, 1438-7492
- Zhu, Z.K.; Yin, J.; Cao, F.; Shang, X.Y. & Lu, Q.H. (2000). Photosensitive polyimide/silica hybrids. *Adv. Mater.*, 12, 14, 1055-1057, 0935-9648

IntechOpen

IntechOpen



Nanomaterials

Edited by Prof. Mohammed Rahman

ISBN 978-953-307-913-4

Hard cover, 346 pages

Publisher InTech

Published online 22, December, 2011

Published in print edition December, 2011

The book "Nanomaterials" includes all aspects of metal-oxide nano-structures, nano-composites, and polymer materials instigating with materials survey and preparations, growth and characterizations, processing and fabrications, developments and potential applications. These topics have utilized innovative methods of preparation, improvement, and continuous changes in multidimensional ways. The innovative frontiers are branching out from time to time to advanced nanotechnology. It is an important booklet for scientific organizations, governmental research-centers, academic libraries, and the overall research and development of nano-materials in general. It has been created for widespread audience with diverse backgrounds and education.

How to reference

In order to correctly reference this scholarly work, feel free to copy and paste the following:

Jeong Hyun Yeum, Jae Hyeung Park, Jae Young Choi Jong Won Kim, Sung Kyou Han and Weontae Oh (2011). Polymer/Montmorillonite/Silver Nanocomposite Micro- and Nanoparticles Prepared by In-Situ Polymerization and Electrospaying Technique, *Nanomaterials*, Prof. Mohammed Rahman (Ed.), ISBN: 978-953-307-913-4, InTech, Available from: <http://www.intechopen.com/books/nanomaterials/polymer-montmorillonite-silver-nanocomposite-micro-and-nanoparticles-prepared-by-in-situ-polymerizat>

INTECH
open science | open minds

InTech Europe

University Campus STeP Ri
Slavka Krautzeka 83/A
51000 Rijeka, Croatia
Phone: +385 (51) 770 447
Fax: +385 (51) 686 166
www.intechopen.com

InTech China

Unit 405, Office Block, Hotel Equatorial Shanghai
No.65, Yan An Road (West), Shanghai, 200040, China
中国上海市延安西路65号上海国际贵都大饭店办公楼405单元
Phone: +86-21-62489820
Fax: +86-21-62489821

© 2011 The Author(s). Licensee IntechOpen. This is an open access article distributed under the terms of the [Creative Commons Attribution 3.0 License](#), which permits unrestricted use, distribution, and reproduction in any medium, provided the original work is properly cited.

IntechOpen

IntechOpen